Sub-basalt imaging in the Faeroe-Shetland Basin with large-offset data

Moritz M. Fliedner and Robert S. White

Summary

On two profiles from the Faeroe-Shetland Basin, where Tertiary basalt flows cover an older sedimentary section, we demonstrate that the seismic image of a sub-basalt target can be much improved by using the velocity and reflectivity information contained in the wide-angle wavefield. While conventional short-offset processing provides a detailed image down to the top of the basalt flows, pre-stack depth migration of selected portions of the wide-angle wavefield allows a composite image to be built which reveals the base of the basalt flow and the underlying sedimentary and basement structure. The velocity field derived from wide-angle traveltimes also assists in identifying the geological origin of the imaged structures.

Introduction

Imaging the potentially prospective structures lying beneath thick basalt flows presents a key technical challenge in the Faeroe-Shetland Basin (Fig. 1) as well as in many other areas of active exploration on the European Atlantic frontier and along the South Atlantic and Indian continental margins.

During continental break-up, extensive basaltic lava flows were produced along the north-west European margin and flowed across pre-breakup sedimentary basins (White & McKenzie. 1989; Richardson *et al.* 1999). The basalt flows, with their high seismic velocities, create a major obstacle to imaging the lower-velocity sedimentary structures which underlie them. The highly reflective top of the basalts scatters much of the incident seismic energy. Short-period ringing, simple and peg-leg multiples obscure weak sub-basalt reflections with similar move-out; the high-velocity basalt layer preferentially absorbs the higher frequencies in the incident wavelet, degrading the achievable resolution of a sub-basalt image; and strong ray-bending caused by large seismic velocity variations may distort the sub-basalt image.

Sub-basalt imaging can be improved by using larger offsets than are usually acquired for marine multichannel seismic reflection profiling. Multiples produced between the sea-surface and the top of the basalt layer that contaminate the near-vertical incidence wavefield are absent from the sub-basalt wavefield (Fig. 2) and the amplitudes of wide-angle arrivals

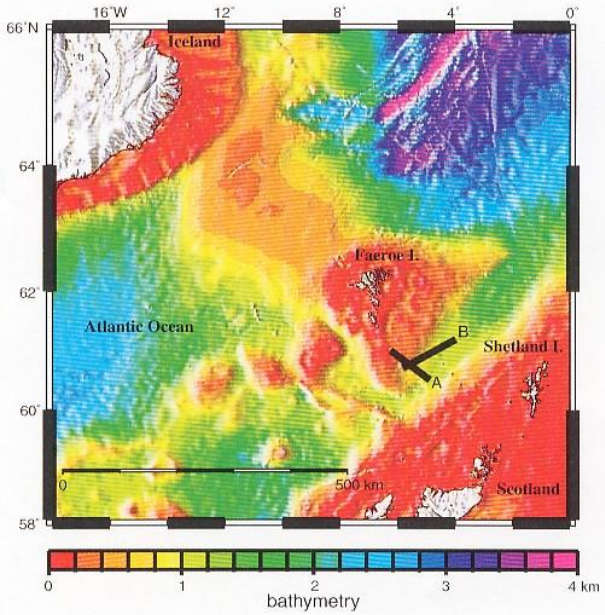

Figure 1 Regional location map showing setting of the Faeroe-Shetland Trough on the continental margin of north-west Europe and the location of the Faeroes Large Aperture Research Experiment (FLARE) profiles discussed in this paper. Profile A is line FLA-4 and profile B is line FLA-7 of the FLARE-1998 data set.

are often large because reflection amplitudes increase towards the critical distance. Seismic velocity control is improved over that conventionally derived from the hyperbolic move-out of short-offset reflections by including inversions of wide-angle reflections and of the traveltimes of diving waves (sometimes called refractions) from the basalt and from deeper high-velocity layers such as the crystalline basement. A reliable sub-basalt velocity model allows direct imaging of the wide-angle wavefield by pre-stack migration to normal incidence. In the following discussion, we use the term 'basement' in a purely functional sense to denote the first bright sub-basalt reflection that exhibits a move-out smaller than that from the base-basalt arrival.

In this paper we show that careful muting and migration of different parts of the seismic wavefield from normal incidence to very wide angles allows different parts of the subsurface to be imaged, with the consequence that a composite image from near-surface sediments to sub-basalt and basement structures can be produced by combining appropriate

Correspondence: University of Cambridge, Bullard Laboratories, Madingley Road, Cambridge UB3 OEZ, UK. E-mail: moritz@esc.cam.ac.uk

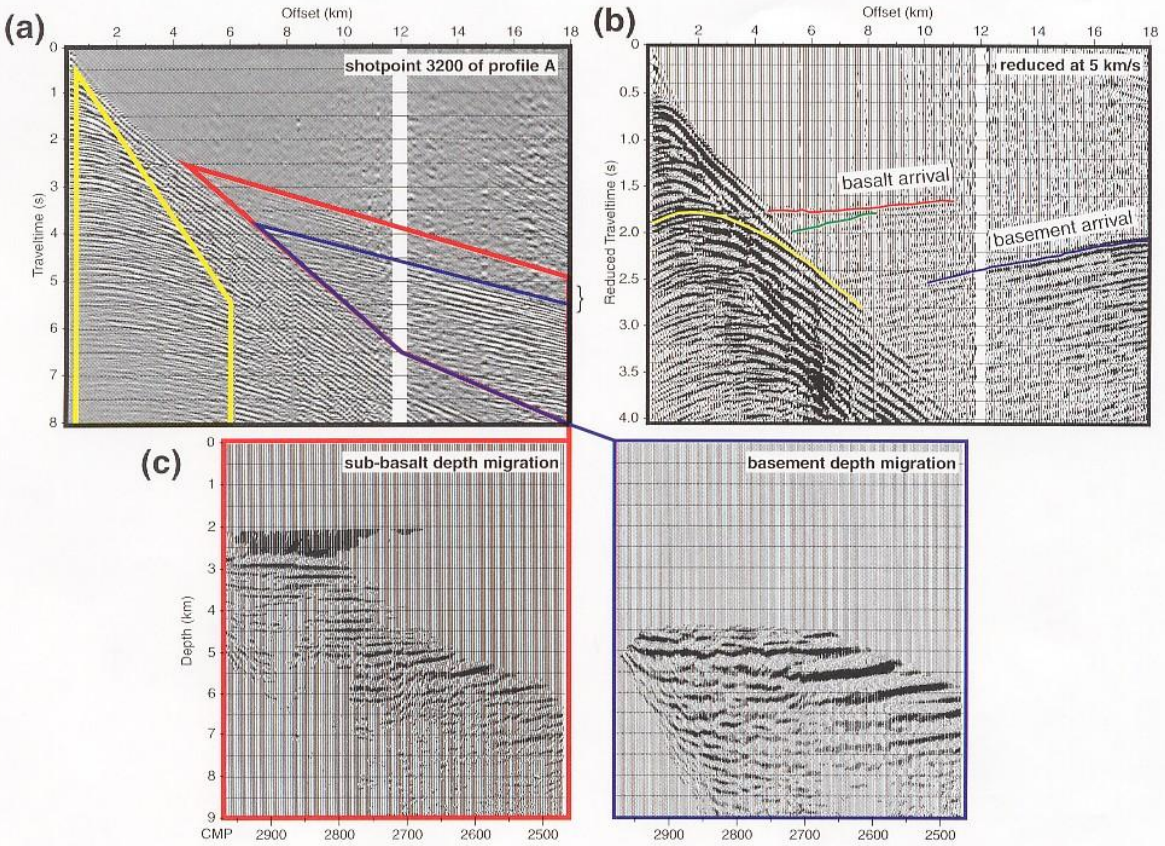

Figure 2 Shot gather 3200 (a) unreduced and (b) reduced at 5.0 km/s. Zero offset is at CMP 3200, offsets increase north-westwards. The main compressional wide-angle arrivals are outlined. (c) Depth migrated wide-angle field of shot 3200. Wavefield used for near-offset processing is framed in yellow, that used for wide-angle sub-basalt processing is framed in red and the portion for wide-angle basement processing is framed in blue. Bracket in (a) marks the step-back from the basalt first arrival (disappearing at an offset of about 14 km) and the basement first arrival that indicates the presence of a sub-basalt low-velocity layer. Arrivals picked for ray-tracing marked on reduced gather (b): yellow – top of basalt reflection, red – basalt diving wave, green – base of basalt reflection, blue – top of basement reflection. All arrivals are marked at the nearest trough for clarity.

migrations of different segments of the total compressional wavefield. We do not deal here with the possibilities of shear-wave imaging that arise from potentially strong mode conversions within the basalt layer. We demonstrate wide-angle P-wave imaging using two crossing profiles, one down-dip (Profile A) and the other at an oblique angle (Profile B), from a grid of long-offset profiles with a two-ship synthetic aperture geometry (White *et al.* 1999) acquired as part of the Faeroes Large Aperture Research Experiment (FLARE). The maximum offset recorded on these two profiles is 18 km, the shot and receiver spacing in the supergathers is 100 m and the sampling rate is 8 ms. The FLARE data set was collected by the Amerada Hess Limited Partner Group (LASMO Limited, Norsk Hydro AS and DOPAS). The two profiles presented in this paper were acquired in 1998 for Amerada Hess Limited by Schlumberger Geco-Prakla in a follow-up to the original 1996 survey (White *et al.* 1999; Fruehn *et al.* submitted) that aimed to explore the whole of the Faeroe shelf prior to the 2000 Faeroese licensing round; 12 profiles were shot altogether.

Velocity modelling of FLARE profiles

A simple inspection of the shot gathers (Fig. 2) reveals the presence of a low velocity layer beneath a high-velocity basalt layer that increases in thickness westward from the centre of the basin towards the Faeroe platform. The underlying low-velocity layer causes a step-back of the wide-angle first arrival at varying offsets along the dip-profile A. We interpret this low-velocity layer as late Mesozoic and possibly earliest Tertiary sediments covered by Tertiary lava flows from the Faeroe Islands that pinch out near the eastern end of the dip-profile A in the centre of the Faeroe-Shetland Trough. This deep sedi-

mentary section is known from the Shetland side of the basin where the section is not covered by lava flows.

Velocity analyses of the near-offset, 6 km streamer data yields a good stacking velocity model for the sediments above the basalt layer, but no reliable information about deeper velocities. We use the interval velocities derived by Dix's equation from the velocity analyses together with picks of the main horizons (seafloor, two sedimentary horizons and top-basalt) from the stacked time section as a starting model to ray trace and invert the main wide-angle arrivals from the supergathers (basalt diving wave, base-basalt reflection, top-basement reflection and, where possible, basement diving wave; fine-tuning of the sedimentary horizons) to derive a velocity model of the deeper layers. We use the ray tracing program 'rayinvr' (Zelt & Smith, 1992) to build the velocity model. Phases were picked on a subset of the available supergathers (Fig. 2b) using every 10th gather, thus producing one source per kilometre.

The velocities in the high-velocity basalt layer are well constrained by the first arrival diving waves, whereas the velocities in the underlying low-velocity zone are constrained only by the top-basement reflection: there is therefore some trade-off between the overburden velocity and the depth to the reflector. Further information on the sub-basalt sediment velocities is derived by extrapolation from velocities determined by conventional means from the area to the east, where the same sediments are not covered by basalt flows. The resulting velocity models (Fig. 3) are the starting models for migration of the wide-angle data. Subsequent migration velocity analyses can then be used iteratively to improve the velocity model. In this study, we used only a single iteration step, which mainly improves the lateral resolution of the two major velocity boundaries at the base of the basalts and the top of the basement.

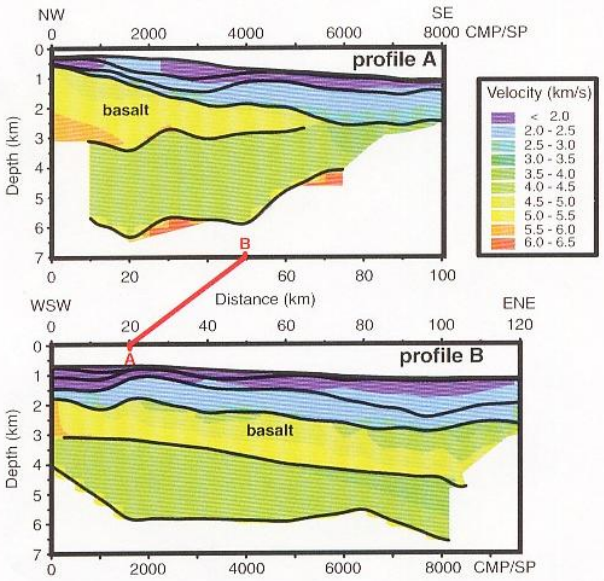

Figure 3 Velocity models of profiles A and B derived by traveltime ray tracing of main refracted and reflected phases. Black, solid lines mark reflecting boundaries; velocity discontinuities are allowed across these boundaries. Intersection of the two profiles marked in red.

Near-offset imaging

The sedimentary structure above the basalt flows is uncomplicated and does not require sophisticated processing before NMO stacking, apart from multiple suppression (Fig. 4). The strong surface-related multiples have been suppressed by Ra-

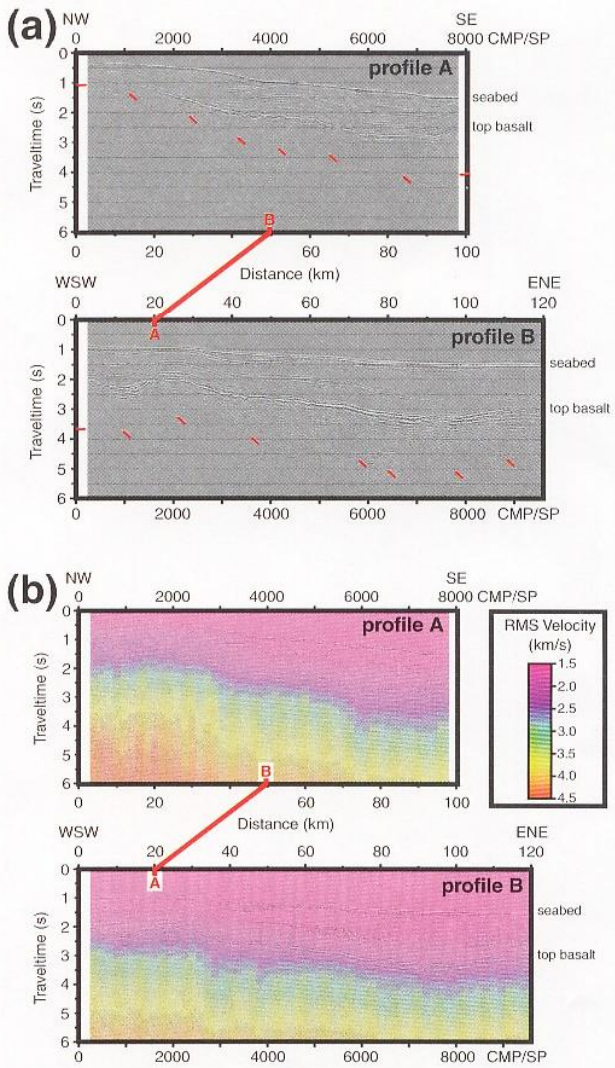

Figure 4 (a) NMO stacks of near-offset data (b) overlaid on RMS (stacking) velocity fields of profiles A and B. Red arrows in (a) mark the top-basalt/seabed/top-basalt multiple.

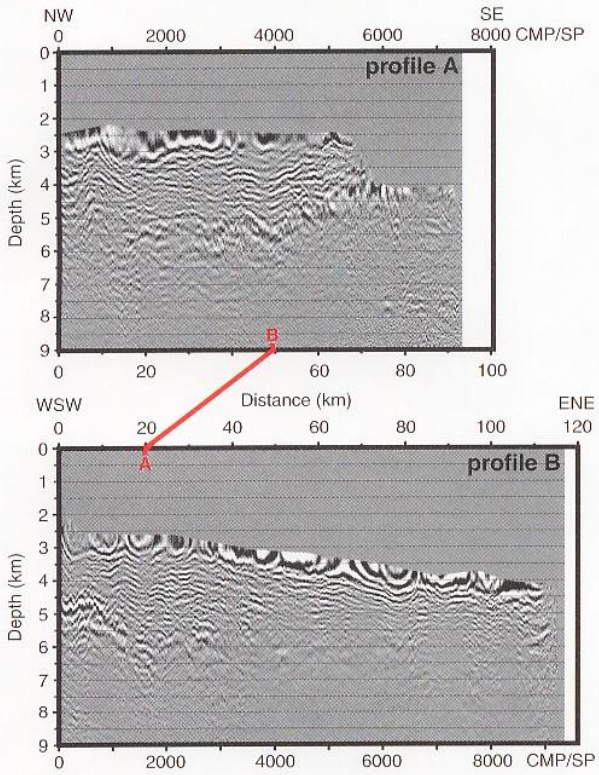

Figure 5 Pre-stack depth migration of compressional wide-angle wavefield. Top mute slightly above the base-basalt reflection showing the basalt refraction that migrates into the basalt layer as it separates from the base-basalt reflection at the nearest wide-angle offsets.

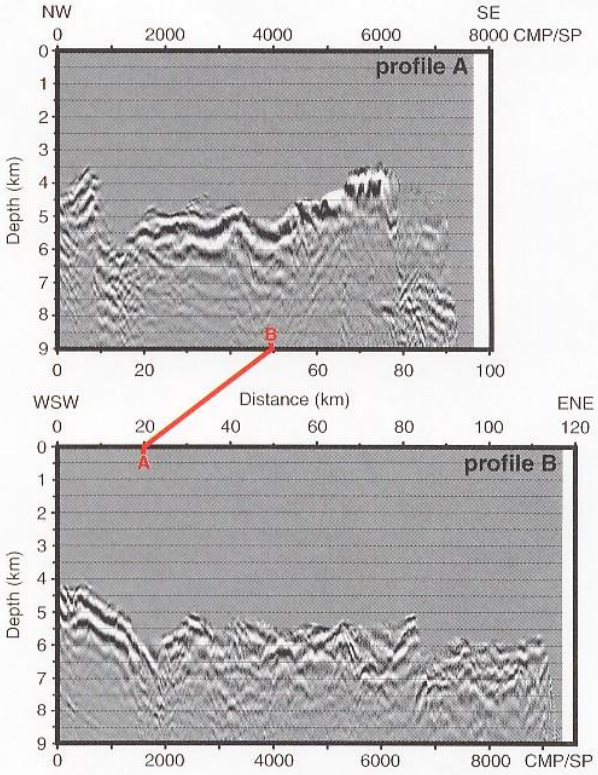

Figure 6 Pre-stack depth migration of compressional wide-angle wavefield muted above the wide-angle basement reflection.

don filtering and inner-trace muting. This leaves nonsurface related multiple paths, most prominently on profile B, but also on profile A where it intersects with B. For example, there is a strong top-basalt/seafloor/top-basalt multiple visible on the near-offset stacks which is absent from the wide-angle data. Primary sub-basalt reflections can be identified in some places, especially on profile B (e.g. CMPs 5000–7000). Clear deep reflections at about 4.3 s, are visible on profile A only at its eastern end beyond the feather edge of the basalt flows (CMPs > 6500).

Wide-angle imaging

The high-velocity basalt layer above the imaging target separates a purely compressional wide-angle wavefield with an asymptotic move-out determined by the basalt P-wave velocity (Haugen & Yu 1998) from the rest of the seismic wavefield, with move-outs up to the highest P-wave velocity reached in the sediments above the basalt flows and the S-wave velocity in the basalts. We exploit this part of the seismic wavefield for imaging by pre-stack depth migration (PSDM; Fig. 2c). Wide-angle data images have an inherently lower frequency content and therefore lower resolution than do normal-incidence data images, due to preferential attenuation of high frequencies and the convergence in time with offset of arrivals that are separate at normal incidence. The result of PSDM on this portion of the wide-angle data is shown in Fig. 5. The basalt arrival disappears as a first (wide-angle) arrival on profile A at CMP 5860 because the basalt layer becomes too thin to be imaged with the wide-angle data. The actual pinch-out point can be determined from the normal-incidence data. As the basement becomes a first arrival, more energy is returned from deeper layers: a group of reflectors at 7–8 km depth are the most prominent arrivals east of CW 6000 on profile A.

The images can be improved by migrating the arrivals from the seismic basement separately (Fig. 6) and merging them with the previous stacks (Fig. 7). This procedure restores approximately the relative peak amplitudes of the main arrivals and allows us to account for the lower frequency content of the deeper arrivals.

Close to the pinch-out of the basalt layer, the basement reflector, which is fairly continuous along most of profile A, becomes weak and gives way to a deeper reflector around 7 km depth as well as a slightly shallower, short reflector between CMP 5500 and 6000. Strong, uncollapsed diffraction tails

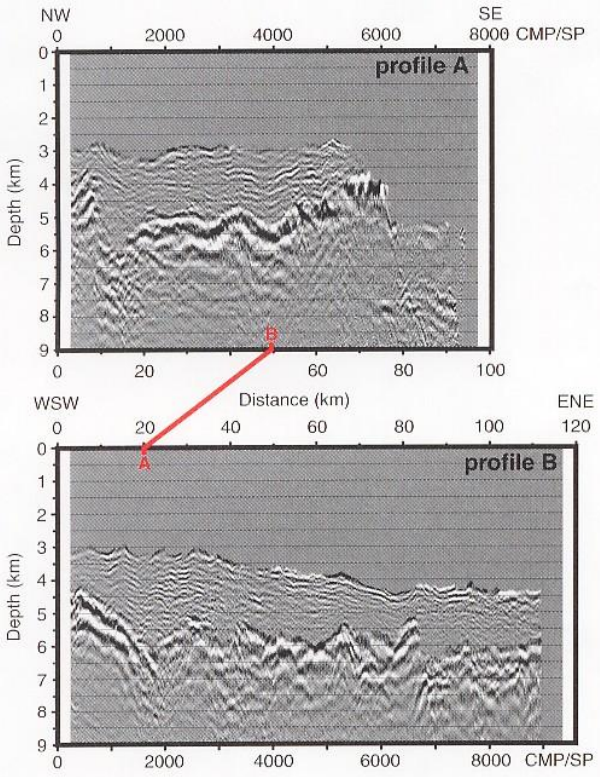

Figure 7 Composite wide-angle images generated by merging Figs 5 and 6.

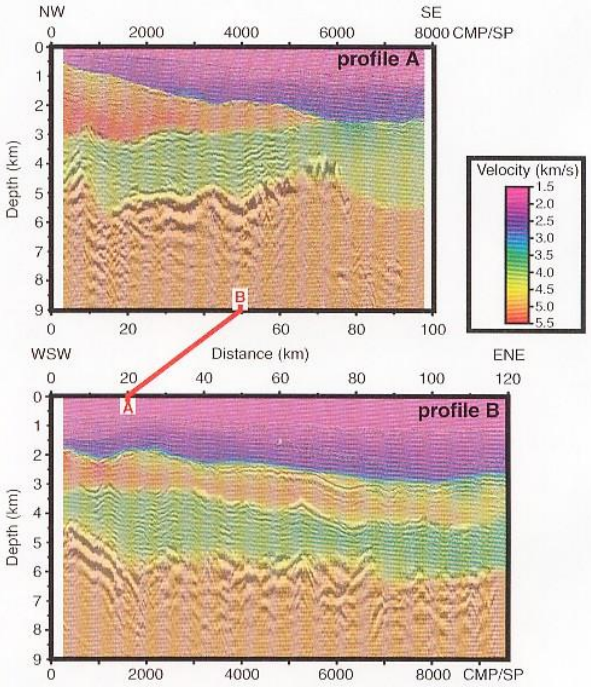

Figure 8 Final composite profiles generated by merging the depth-converted near-offset section of Fig. 4 above the base of basalt with Fig. 7. The seismic image overlays the velocity model used for pre-stack depth migration.

from this reflector indicate that this feature has not been well resolved by the wide-angle migration; it may be a discontinuity in the basement reflector or a sill intruded into the overlying low-velocity zone.

Since the wide-angle images do not contain data above the base-basalt, we merge them with the depth-converted near-vertical time stacks to generate composite depth sections (Fig. 8).

Discussion of the composite depth-sections

The velocity model used for the pre-stack depth migration is far smoother than the seismic image generated with it. This reflects the limitations of ray tracing and traveltime inversion based on manually identified and picked phases from a subset of seismic gathers. It nevertheless clearly delineates the major geological units in the two profiles. In an iterative approach, this velocity model could be refined by migration velocity analysis of the resulting image gathers.

The base of the basalt flows is considerably more rugged than that expected from the velocity model, and the image quality varies accordingly. The best focusing was achieved on relatively smooth stretches between CMPs 1500 and 3200 on profile A and CMPs 5000 and 6600 on profile B. The relief of the base of the basalt flows does not follow the basement relief closely since the basement was already covered by sediments before the basalts were emplaced over them. The thickness of the sub-basalt low-velocity zone interpreted as sediments varies by a factor of three along profile B from a minimum of less than 1 km at CMP 6500 to a maximum of almost 3 km at CMP 1700 near the intersection with profile A. At least two distinct seismic units can be distinguished in the sedimentary low-velocity zone on profile A: a drape of reflectors over the basement high at CMP 700 separated from more flat-lying reflectors to the east by an east-dipping reflector of strongly variable amplitude that reaches the base of the basalts at CMP 1500 and the basement at CMP 3200.

The basement is well imaged between CMPs 1300 and 4500 on profile A and CMPs 300 and 1700 on profile B. The variable and discontinuous basement topography suggests the presence of tilted fault blocks that produce strong reflections whenever their faces are orientated favourably towards the incident wide-angle rays. The interpretation of the basement is complicated by the fact that large sills may produce wide-angle reflections that look like genuine basement reflections except for their smaller lateral extent. We suspect the presence of such sill reflections in at least two places. On profile A, the 'basement' reflector seems to be isolated between CMPs 5300

and 6100 at 4 km depth while a weak continuous reflector can be seen about 1 km deeper. On profile B, the west-dipping reflector between CMPs 6200 and 6700 at 6–5.5 km depth does not continue eastwards, and even the near-offset image of Fig. 4 shows here a reflector that clearly cuts across the general trend of the reflectivity, which deepens slightly to the east.

The first bright sub-basalt reflector, which we have generically called 'basement', in general obscures any deeper reflectivity. At the south-eastern end of profile A where there are no basalt flows, however, the basement becomes a relatively weak first arrival at wide angles and reveals a much stronger, deeper reflector at a depth of 7.5 km. It is unclear how this reflector continues westward of CMP 5900: it may be continuous with an east-dipping reflector that separates from the basement reflector at CMP 1600 at 6 km depth and remains clearly visible down to a depth of 6.5 km at CMP 2200 and can tentatively be traced further to a depth of 7.5 km at CMP 4200. An interpretation of this reflector is difficult, because no reliable velocity information is available from these depths.

Conclusion

Careful use of the information carried by different parts of the seismic wavefield can produce a composite image that is far superior to those generated either from conventional near-offset data or solely from wide-angle data. In particular, we have shown that in the Faeroes-Shetland Basin careful processing of seismic data that extend from normal incidence to very large offsets is capable of producing composite seismic sections that image not only the top and base of the basalt flows, but also the underlying sedimentary and basement structure. The improvement in imaging is clearly demonstrated by comparison between the final composite sections in Fig. 8 and the conventional reflection section in Fig. 4.

A further advantage of using a large range of offsets is that support for the geological interpretation is provided by the independent information carried by the seismic velocity field in addition to the seismic image. In Fig. 8 we superimpose the seismic image on the coloured velocity background to demonstrate the ability of the velocities to 'tag' the main reflectors and hence to assist in the identification of their geological origin. On a finer scale, detailed studies of the AVO characteristics of reflections at very wide angles may also assist in constraining the rock types responsible for particular reflectors (Fliedner & White, submitted).

Acknowledgements

We are grateful to Amerada Hess UK Limited for permission to use their data. We acknowledge our collaborators from the FLARE partners, LASMO Limited, Norsk Hydro AS and DOPAS (now DONG), and particularly Ed Cullen, Wayne Kirk, John Smallwood and Chris Latkiewicz of Amerada Hess UK Limited. The opinions and interpretations expressed herein are those of the authors and not necessarily those of Amerada Hess Limited. We thank the reviewer Matt Luheshi for his comments. Department of Earth Sciences. Cambridge contribution number 6282.

References

Fliedner, M.M. and White, R.S. [submitted] Seismic structure of basalt flows from surface seismics, borehole measurements and synthetic seismogram modeling. *Geophysics*.

Fruehn, J., Fliedner, M.M. and White, R.S. [submitted] Integrated wide-angle and near-vertical sub-basalt study on large aperture seismic data from the Faeroe-Shetland region. *Geophysics*.

Haugen. G.U. and Yu. F. [1998] Can seismic wide-aperture data image beneath basalt? 68th Annual International Meeting. Society Expl. Geophys, Expanded Abstracts, 90–93.

Richardson, K.R., White, R.S., England, R.W. and Fruelm. J. [1999] Crustal structure east of the Faroe islands: mapping sub-basalt sediments using wide-angle seismic data. *Petroleum Geoscience* 5, 161–172.

White, R.S., Fruehn, J., Richardson, K.R., Cullen, E., Kirk, W., Smallwood, J.R. and Latkiewicz, C. [1999] Faeroes Large Aperture Research Experiment (FLARE): imaging through basalts. In: *Petroleum Geology of Northwest Europe: Proceedings of the 5th Conference* (Fleet, A.J. and Boldy, S.A.R., eds), pp. 1243–1252. Geological Society, London.

White, R. and McKenzie, D. [1989] Magmatism at rift zones: The generation of volcanic continental margins and flood basalts. *Journal of Geophysical Research* **94**(B6), 7685–7729.

Zelt, J.A. and Smith, R.B. [1992] Seismic traveltime inversion for 2-D crustal velocity structure. *Geophysical Journal International* **108**, 16–34.